An Age-Structured Model for Erythropoiesis using Hematocrit

Joseph M. Mahaffy,*Samuel W. Polk,†and Roland K. W. Roeder‡
Department of Mathematical Sciences
San Diego State University
San Diego, CA 92182-0314

October 31, 2023

Abstract

This study examines an age-structured model for erythropoiesis using hematocrit to control EPO production. The model extends previous work to include the variable velocity of maturation along with the effects of blood plasma on hematocrit. Experimental data on phlebotomized subjects are used to fit the parameters in the model, and various numerical simulations are performed. The numerical studies are compared to previous models for humans following a blood donation and rabbits with an induced autoimmune hemolytic anemia. Numerical simulation of the age-structured model allows important comparisons to blood reticulocyte experiments. The variable aging of precursors to erythrocytes results in increased stability of the model, indicating that this may be an important adaptive control. The relative importance of the various controls in the model and their physiological significance are discussed. Experimental hematocrit readings on two of the authors suggest more complicated controls.

Key words: age-structured model, erythropoiesis, hematocrit, phlebotomy, autoimmune hemolytic anemia, state-dependent delay differential equations, method of characteristics, numerical simulations

*The work of this author was supported in part by NSF grant DMS-9208290 and Centre de recherches mathématiques, Université de Montréal, Montréal, Québec H3C 3J7.

†The work of this author was supported under the MARC/RCMS program of NIH by grant 5-34-GM08303-04.

‡The work of this author was supported under the REU program of NSF by grant DMS-9208290.

1 Introduction

The advent of the serious disease AIDS has caused great concern about the HIV virus infecting the blood supplies around the world. Each day 40,000 units (450 g) of blood are needed in the U.S. [1], yet no artificial substitute has been created. This means that blood donations remain a critical life-giving source for the many operations and replacements needed after massive hemorrhages from accidents or treatment of diseases like hemophilia. A better understanding of the regulation of erythropoiesis through modeling may provide valuable information on optimal collection schemes for autologous donors who want to guarantee a safe blood supply or help increase supplies in the case of a major disaster.

There are several hematopoietic diseases that are believed to arise due to abnormalities in the feedback controls regulating hematopoiesis [8, 17, 18, 19, 21, 22, 23, 24, 29, 36, 43, 45, 46, 47]. For example, oscillations in the erythrocyte concentrations are observed in cases of autoimmune hemolytic anemia [13, 31, 33]. An age-structured model of Bélair *et al.* [2] and Mahaffy *et al.* [26] reasonably reproduced the experimental results of Orr *et al.* [31] for rabbits that were given red blood cell iso-antibodies over a long period of time, inducing an autoimmune hemolytic anemia. The mathematical models provide an alternate tool for understanding the relative importance of the different physiological controls and could be used to test therapeutic treatments.

Erythropoiesis is the genesis of undifferentiated stem cells, primarily in the bone marrow, to mature red blood cells, or erythrocytes, which circulate throughout the body to deliver oxygen (O_2) to the tissues. (*William's Hematology* [4] provides an excellent reference for erythropoiesis.) The primary control of erythropoiesis is governed by the hormone erythropoietin (EPO), which is released in the bloodstream based on a negative feedback mechanism that detects the partial pressure of O_2 in the blood. The concentration of EPO directly affects precursor cells (BFU-Es and CFU-Es) by determining the number that mature into erythrocytes through either recruitment or preventing apoptosis. In addition, EPO appears to accelerate the maturing process when the hematocrit is particularly low.

The regulation of erythropoiesis has been studied extensively using age-structured models [2, 5, 6, 7, 14, 15, 26, 27]. Bélair *et al.* [2] and Mahaffy *et al.* [26] used several assumptions to reduce their age-structured models to models with delays that allowed bifurcation analysis and relatively simple numerical studies. This work extends the mathematical model developed in Mahaffy *et al.* [26] to include the effects of blood plasma on the regulation of

erythropoiesis following a phlebotomy. After a phlebotomy, the body loses both erythrocytes and plasma. However, the O_2 detection, which determines the quantity of EPO released, probably depends on the concentration of hemoglobin in the blood. The model of Mahaffy *et al.* [26] is modified to examine the concentration of hemoglobin, then numerical studies find parameter values that best fit the experimental studies of Maeda *et al.* [25] and Wadsworth [42] for a collection of normal males following a phlebotomy.

The complete age-structured model includes a variable velocity of aging for the precursor cells, which has been observed experimentally ([4], p.436). This effect significantly increases the difficulty of study, as the model no longer reduces to a relatively simple system of delay differential equations. Bélair and Mahaffy [3] linearized the age-structured model and demonstrated how varying the velocity of aging stabilizes a similar model. Simulation of the partial differential equations allows the mathematical model to be compared to experimental studies on reticulocytes in the blood, which physiologists use to gauge new erythrocyte production. To analyze a variable velocity of aging, the system of partial differential equations is simulated numerically. Our numerical studies use a modification of the method of characteristics presented by Sulsky [39, 40] for age-structured models and compare the results to the simplified model discussed above. Our analysis of the mathematical model simulating the experiment of Orr *et al.* [31] for an induced autoimmune hemolytic anemic in rabbits shows that creating the initial data for the system of delay differential equations is fairly complex compared to the initial conditions for the partial differential equations. However, the partial differential equation code is significantly more complex and requires smaller stepsizes for a given accuracy. These numerical results reinforce the analytical results of Bélair and Mahaffy [3], showing that inclusion of a variable velocity of aging for precursor cells stabilizes the mathematical model and suggesting the importance of this adaptation to physiological controls.

In the next section we briefly present crucial elements of the physiology used to formulate the age-structured model, including the changes from the previous age-structured models of Bélair *et al.* [2] and Mahaffy *et al.* [26]. Several assumptions are necessary to reduce the age-structured model to a system of state-dependent delay differential equations. The third section begins with a least squares best fit of the simplified delay differential equation model to the collective experimental data of normal males following a phlebotomy. A numerical scheme based on the method of characteristics is developed to study the complete age-structured model, including the complication caused by a variable velocity of aging. By examining the pop-

ulations in the lower age classes, the mathematical model can simulate the experimental studies of blood reticulocytes, giving an indirect measure of erythrocyte production. When the velocity of aging of the precursor cells is allowed to vary, the numerical simulations show increased stability of the model. We improve on earlier models of a rabbit with an induced autoimmune hemolytic anemia [2, 26] by using hematocrit for the control and including additional modifications on rabbit physiology from the literature. A linear analysis of the models proves the stabilizing effects of a variable velocity of aging by precursor cells. Numerical studies give an error analysis of the computer algorithms that are employed. The final section contains actual data collected on two of the authors following a phlebotomy, and these data show additional complications in the physiological controls for the concentration of erythrocytes in the blood. We discuss the relevance of our mathematical model to normal subjects following a phlebotomy and to diseased states, such as a hemolytic anemia.

2 Mathematical Model using Hematocrit

This section summarizes key elements in the physiology of erythropoiesis and develops a mathematical model describing this process, especially following a significant blood loss. The model and its associated assumptions closely parallel the earlier works of Bélair *et al.* [2] and Mahaffy *et al.* [26]. After a phlebotomy, the body has lost about 450 g of whole blood, which is about 7-8% of total blood volume for the average man. About 43% of the blood by volume ([4], p.426) is erythrocytes with most of the remainder being plasma. The plasma is replaced fairly rapidly; however, the erythrocytes require the much longer process of erythropoiesis to regenerate. Since biological controls usually react to concentration changes, the model developed here differs from the earlier models by examining the hematocrit or hemoglobin concentration instead of the direct population of erythrocytes. This requires the addition of a function for the plasma component in whole blood.

Since this model extends earlier models [2, 26], we significantly condense the physiological information used to develop the age-structured model. Erythropoiesis begins with either the pluripotential stem cell or a self-sustaining pool of BFU-Es (burst forming units already committed to become erythrocytes). The precursor cells rapidly proliferate, primarily under the influence of the hormone erythropoietin, EPO, for about 4 days until they become

reticulocytes. The reticulocytes spend a couple more days increasing their hemoglobin content, becoming more specialized, and shrinking in size. The reticulocytes enter the blood stream, then after 1-3 days lose their nucleus and become mature erythrocytes. Erythrocytes are specialized cells containing hemoglobin that transport O_2 from the lungs to the other tissues in the body. Specific cells, primarily the peritubular interstitial cells of the outer cortex in the kidneys, sense the partial pressure of O_2 in the blood and release EPO using negative feedback to complete this physiological control loop.

Since the process of erythropoiesis depends on the relatively long maturation and finite life-span of the erythrocytes, an age-structured model provides a natural means of studying this population of cells. The age-structured model begins with the population of precursor cells, denoted $p(t, \mu)$, where t is the simulation time and μ is the age of the precursor cells and could represent accumulation of hemoglobin. Experiments suggest that EPO affects the early stages of erythropoiesis in two significant ways. Its primary control is on the number of new cells recruited into the proliferating precursor population, probably by preventing apoptosis of CFU-Es. Let $S_0(E)$ represent the number of new precursor cells, which are recruited and survive into the proliferating precursor cell population. EPO also appears to accelerate the maturing process, so let $V(E)$ be the velocity of maturation. This information combines to give the boundary condition:

$$V(E)p(t, 0) = S_0(E). \tag{2.1}$$

In general, the birth rate for the proliferating precursor cells depends on the level of maturity, μ, and the concentration of EPO and is denoted $\beta(\mu, E)$. If $\kappa(\mu - \bar{\mu})$ is the distribution of maturity levels of the cells that are released into the circulating blood, where $\bar{\mu}$ represents the mean age of mature precursor cells (reticulocytes) and μ_F is the maximum age of a precursor cell, then

$$\int_0^{\mu_F} \kappa(\mu - \bar{\mu}) d\mu = 1,$$

and the disappearance rate function is given by:

$$\mathcal{K}(\mu) = \frac{\kappa(\mu - \bar{\mu})}{\int_\mu^{\mu_F} \kappa(s - \bar{\mu}) ds}.$$

Experiments of Finch *et al.* [10] show that following a significant blood loss, there is an early release of stored reticulocytes, called "shift reticulocytes."

Thus, a better model might have $\mathcal{K}$ depend on either EPO or the concentration of mature cells. Our $V(E)$ partially accounts for this phenomenon. With these conditions the age-structured model for the population of precursor cells with $t > 0$ and $0 < \mu < \mu_F$ satisfies:

$$\frac{\partial p}{\partial t} + V(E)\frac{\partial p}{\partial \mu} = V(E)[\beta(\mu, E)p - \mathcal{K}(\mu)p]. \tag{2.2}$$

The last stage of development for precursor cell is the non-proliferative phase, where the cells now called reticulocytes become packed with hemoglobin and lose many other cellular components. The reticulocytes squeeze out of the bone marrow and enter the blood stream, where they soon become mature erythrocytes, which transport O_2 to the tissues of the body. Let $m(t, \nu)$ be the population of erythrocytes in the blood at time t and age ν. If the mature cells age at a rate W, which is almost constant for erythropoiesis since the aging process appears to depend only on the number of times that an erythrocyte passes through the capillaries, then the boundary condition for cells entering the mature population is given by the following expression:

$$Wm(t, 0) = V(E)\int_0^{\mu_F} \kappa(\mu - \bar{\mu})p(t, \mu)d\mu. \tag{2.3}$$

Note that the earliest age classes of the mature population actually represent blood reticulocytes.

After many times of being squeezed through the capillaries, the oldest erythrocytes lose pliability of their membranes, which cannot be repaired without a nucleus. Since these cells could cause damage to the circulatory system by blocking blood vessels, the oldest erythrocytes are marked for active degradation by macrophages. Assuming either a constant supply of markers or number of phagocytes that are satiated from engulfing the oldest erythrocytes results in a constant flux of erythrocytes from the mature population. This produces a moving boundary condition with the age of the oldest erythrocyte, $\nu_F(t)$, varying in t. The boundary condition, following Mahaffy *et al.* [26], is given by:

$$(W - \dot{\nu}_F(t))m(t, \nu_F(t)) = Q, \tag{2.4}$$

where Q is the fixed erythrocyte removal rate. A number of erythrocytes from all age classes are lost primarily from the breakage of capillaries due to body movement or physical impact such as that caused by feet hitting a hard surface while running. Let $\gamma(\nu)$ be the death rate of mature cells

(depending only on age), then the age-structured model describing $m(t,\nu)$ is given by:

$$\frac{\partial m}{\partial t} + W\frac{\partial m}{\partial \nu} = -W\gamma(\nu)m, \quad t > 0, \quad 0 < \nu < \nu_F(t), \tag{2.5}$$

where the maximum age, $\nu_F(t)$, is determined by (2.4).

The ability of blood to carry O_2 to the tissues is more complicated than the simple counting of erythrocytes in the blood. A standard phlebotomy for a normal male entails a 7-8% loss in total blood volume with 43% of that volume on average being erythrocytes. (Females have a lower average hematocrit with greater variability due to their body tissue composition and menstrual cycle and lose a higher percentage of blood volume from their smaller size. [28]) The initial response of the body is to shunt blood away from less important tissues, which means vital organs such as the kidneys where the majority of the O_2 sensors reside will see no significant drop in the partial pressure of O_2. There are O_2 sensors in the skin from which the blood is shunted, but our model does not consider this. A better measure of the O_2 carrying ability of the blood and the test used by blood banks is the concentration of hemoglobin, which is the actual O_2 carrying molecule. Another related quantity is the hematocrit, which is the percent of the blood volume comprised of erythrocytes. Since the concentration of hemoglobin in erythrocytes is almost constant, there is a strong correlation between these measurements. Thus, the blood's O_2 carrying capacity is directly related to the hematocrit, $H(t)$, or hemoglobin, $Hb(t)$, which are given by:

$$H(t) = \frac{M(t)}{M(t)+q(t)} \qquad \text{and} \qquad Hb(t) \simeq \tfrac{100}{3}H(t), \tag{2.6}$$

where $M(t)$ is the total volume of erythrocytes and $q(t)$ is the plasma volume. With the assumption that all erythrocytes are similar in volume, independent of age, the erythrocyte volume correlates directly to the total population of mature cells, so

$$M(t) = \int_0^{\nu_F(t)} m(t,\nu)d\nu, \tag{2.7}$$

and M has volume units equivalent to the average size of the erythrocyte.

The plasma volume is more rapidly generated. First, interstitial fluid enters blood vessels to increase blood volume, then with hydration the blood generates new serum proteins with significant increases in liver albumin synthesis after 36 hr, creating new plasma. Moore [28] states that following a

large blood loss, plasma begins entering the blood on average at 40-60 ml/hr and stabilizes exponentially in 30-40 hr. This blood volume change occurs primarily at the expense of the interstial volume, which takes several days to recover. The data of Wadsworth [42] suggests that the new plasma increases blood volume to a level higher than before the phlebotomy. From these data, we chose the plasma function

$$q(t) = \alpha_1(1 + (\alpha_2 t - 0.08)e^{-\alpha_3 t}), \tag{2.8}$$

where 0.08 reflects the plasma lost at $t = 0$ (time of the phlebotomy) and α_1 normalizes the plasma volume with the erythrocyte volume M. The parameters α_2 and α_3 are found in the next section using a least squares best fit to the data of Maeda *et al.* [25] and Wadsworth [42].

The EPO level E is governed by a differential equation with a negative feedback, depending on the hematocrit, $H(t)$, or hemoglobin, $Hb(t)$, which reflects O_2 carrying capacity of the blood. Since most data give the concentration of hemoglobin, the equation used in our model for human subjects is given by

$$\frac{dE}{dt} = f(Hb) - kE, \tag{2.9}$$

where k is the decay constant for the hormone and $f(Hb)$ is a monotone decreasing function of Hb, representing the negative feedback effect of the O_2 carrying capacity of the blood on the rate of hormone production. We choose the Hill function f:

$$f(Hb) = \frac{a}{1 + K(Hb)^r}, \tag{2.10}$$

which often occurs in enzyme kinetic problems. For our simulations on rabbits with an induced hemolytic anemia, we substitute $H(t)$ for $Hb(t)$ in f. Bélair *et al.* [2] used experimental data in the literature to find the parameter r, while the parameters a and K are found in the beginning of the next section by a least-squares estimate.

Mahaffy *et al.* [26] analyzed the partial differential equations and their boundary conditions given by Eqns. (2.1)–(2.5), which describe an age-structured model for the erythrocytes. The method of characteristics is applied to this system following the techniques of several authors [2, 11, 12, 26, 27, 37] to produce a system of threshold delay equations. The method of characteristics is also the basis of the numerical scheme for solving the partial differential equations in the next section.

In their general form, Eqns. (2.1)–(2.9) are too complicated to analyze and fit to experimental data. Mahaffy *et al.* [26] made several simplifying

assumptions that are reasonable for erythropoiesis, which allowed reduction of the system of threshold delay equations to a system of delay differential equations with a fixed delay in one equation and a state dependent delay in an equation governing the age at which mature erythrocytes die. Our analysis of the age-structured model for erythropoiesis following a phlebotomy begins with very similar assumptions to fit the experimental data and connect to the previous research [2, 26], then it relaxes the condition on the velocity of aging to better match known effects of EPO and determine how much this affects the model through computer simulation.

Following Mahaffy *et al.* [26] for the simplified model, we assume that the velocities of aging are constant and normalized to one, *i.e.,*

$$V(E) = 1 \qquad \text{and} \qquad W = 1.$$

This assumption significantly simplifies the expressions for $p(t, \mu)$ and $m(t, \nu)$. The second assumption is that the precursor cells grow exponentially for a given period of time μ_R, then stop dividing as seen in the physiological system. This assumption on the birth rate of the precursor cells yields

$$\beta(\mu, E) = \begin{cases} \beta, & \mu < \mu_R, \\ 0, & \mu \geq \mu_R, \end{cases} \tag{2.11}$$

for some constant growth rate β. If $\kappa(\mu - \bar{\mu})$ is a Dirac δ-function, then the changing of precursor cells into mature erythrocytes only occurs on the boundary. Finally, the death rate of the mature cells, $\gamma(\nu)$, is taken to be constant. From Mahaffy *et al.* [26], these assumptions reduce the age-structured model to the following system of delay differential equations with a fixed delay T and a state dependent delay occurring in the equation governing the age at which mature cells die:

$$\begin{aligned} \frac{dM(t)}{dt} &= e^{\beta\mu_R} S_0(E(t-T)) - \gamma M(t) - Q, \\ \frac{dE(t)}{dt} &= f(Hb(t)) - kE(t), \\ \frac{d\nu_F(t)}{dt} &= 1 - \frac{Qe^{-\beta\mu_R} e^{\gamma\nu_F(t)}}{S_0(E(t-T-\nu_F(t))}. \end{aligned} \tag{2.12}$$

Note that $Hb(t)$ in the second differential equation is found by Eqns. (2.6) and (2.8).

As noted in Mahaffy *et al.* [26], the system of equations (2.12) is relatively easy to analyze. The first two differential equations are uncoupled from the

state-dependent delay in the $\dot{\nu}_F(t)$ equation. Thus, bifurcation analysis is reduced to examining a system of two differential equations with a single time delay, T. Furthermore, this system of delay differential equations is readily simulated using an adaptation of the fourth order Runge-Kutta for ordinary differential equations. This latter fact significantly simplifies our problem of fitting parameters in the model to the experimental data.

3 Numerical Simulation of the Model

The model derived in the previous section was developed to examine the controls of the erythropoietic system based on hematocrit, rather than the population of erythrocytes found in previous models [2, 26]. Blood banks require eight weeks between blood donations, but could a more optimal strategy be developed for crisis periods requiring increased blood supplies or could autologuous donors wanting the safety of their own blood during optional surgery obtain a larger supply? Several experiments have collected data on hemoglobin and EPO concentrations for human subjects following a phlebotomy. To test the age-structured model developed in the previous section, we need data over several weeks, so the data of Maeda *et al.* [25] and Wadsworth [42] were combined. These data and some physiological information were sufficient to identify the many parameters in the simplified model (2.12) using a least squares best fit. The model fits the collection of data reasonably well, so could be used to examine different blood donation schemes without human subjects. However, the significant variation observed in individual data (as shown in the next section) suggests additional factors be considered.

The studies of (2.12) are extended to test the effects of the state varying velocity $V(E)$, which is the key complicating element preventing the reduction of the threshold-type delay differential equations to the simplified system of delay differential equations (2.12). Sulsky [39, 40] showed that one of the most efficient numerical methods for age-structured models uses the method of characteristics, which is how our age-structured model (2.1)–(2.9) is simplified. When her models included mass-structure [40], which is similar to our model with the state varying velocity, then a combination of the method of characteristics with an adaptive grid scheme was the best numerical routine that she tested.

The numerical studies examine how the variable velocity of aging of precursor cells affect the stability of our model of a phlebotomy, then they

are extended to a case study of a rabbit with an induced hemolytic anemia. In this second case, the variable velocity of aging is shown to have a significant stabilizing effect. The physiological parameters for the rabbit are improved over earlier studies [2, 26] and include the negative feedback based on hematocrit. Linearization of the functional differential equations about the unique equilibrium of the general model and analysis using the characteristic equation provide details on how the variable velocity stabilizes the model. Also, an error analysis is presented on the convergence of the numerical simulations.

3.1 Parameter Estimation for Normal Human Subjects

The analysis of the mathematical model begins with identification of the parameters for a normal human male following a phlebotomy. The simplified system of delay differential equations (2.12) with the plasma function (2.8) and nonlinear feedback function (2.10) has twelve parameters and the function $S_0(E)$ to be determined. Bélair *et al.* [2] and Mahaffy *et al.* [26] used information about the human erythropoietic system to find many of the parameters. From cell doubling times and the average time for precusor cells to reach the stage of reticulocytes, $\beta = 2.079$ (da^{-1}) and $\mu_R = 4.0$ (da). The average loss of erythrocytes, not caused by aging, is assumed to be $\gamma = 0.001$ (da^{-1}). The average time of maturation gives $T = 6$ (da), while the average mature cell lives 120 (da), which is the equilibrium value for ν_F.

Since a normal human subject has 3.5×10^{11} erythrocytes/kg of body weight [9], we assumed the equilibrium value of $\overline{M} = 3.5$. From Maeda *et al.* [25], we assumed the initial and equilibrium value of EPO to be 16.95 (mU/ml), while the combined experimental data gave an equilibrium for the concentration of hemoglobin, $\overline{Hb} = 15.29$ (g/100 ml). With (2.6) and (2.8), the values of $\overline{M}$ and $\overline{Hb}$ give $\alpha_1 = 4.13$. With the parameter and equilibrium values listed above and the assumption that $S_0(E)$ is linear, then a steady-state analysis of (2.12) yields $S_0(E) = 4.466 \times 10^{-7} E$ and $Q = 0.02745$. Bélair *et al.* [2] found that the Hill coefficient in (2.10) is $r = 6.96$.

The information above provides all parameters for the simplified model (2.12), except for $\boldsymbol{\alpha} = (\alpha_2, \alpha_3, a, K)$ and k in Eqns. (2.8) and (2.10). The parameter k relates to the half-life of EPO, which literature gives values ranging from 4 to 24 hr, and is computed from the equilibrium conditions on the second equation in (2.12). The four parameters, $\boldsymbol{\alpha}$, have no direct biological interpretation, so they were fit to the Maeda *et al.* [25] and Wadsworth [42] data on normal human subjects following a phlebotomy using a least

squares functional. The Maeda *et al.* [25] data on EPO concentration have error bars that are ten times the error bars for their hemoglobin concentration. Thus, we chose to give the EPO data only 10% the weighting of the hemoglobin data. Let $Hb_d(t_i)$ and $E_d(t_i)$ be the average hemoglobin and EPO concentrations, respectively, of the human subjects at day t_i and $Hb(t_i, \boldsymbol{\alpha})$ and $E(t_i, \boldsymbol{\alpha})$ be the solutions of (2.12) depending on the parameters $\boldsymbol{\alpha}$. If $\overline{Hb} = 15.29$ and $\overline{E} = 16.95$ are used to normalize the data, then the least squares functional to be minimized is given by

$$
\begin{aligned}
(3.1)\, J(\boldsymbol{\alpha}) \;\; = \;\; & w_m \sum_{i=1}^{N_m} \left(\frac{(Hb_d(t_i) - Hb(t_i, \boldsymbol{\alpha}))^2}{\overline{Hb}} + 0.1 \frac{(E_d(t_i) - E(t_i, \boldsymbol{\alpha}))^2}{\overline{E}} \right) \\
& + w_w \sum_{i=1}^{N_w} \left(\frac{(Hb_d(t_i) - Hb(t_i, \boldsymbol{\alpha}))^2}{\overline{Hb}} \right),
\end{aligned}
$$

where $w_m = 8$ and $w_w = 7$ are the numbers of subjects in the Maeda *et al.* [25] and Wadsworth [42] data, respectively, and N_m and N_w are the number of times data were collected. The functional (3.1) was minimized by a computer search over a range of parameter values. For each set of values $\boldsymbol{\alpha}$, a modified Runge-Kutta scheme was used to simulate (2.12), then the value of (3.1) was computed and compared to other values of $\boldsymbol{\alpha}$. Fig. 3.1 shows the data with the solution $Hb(t)$ to (2.12) with the optimal parameter values, $\alpha_2 = 0.05332$, $\alpha_3 = 0.09872$, $a = 184.6$, and $K = 9.238 \times 10^{-9}$. The values of α_2 and α_3 are reasonable based on the information given by Moore [28] and Wadsworth [42]. The equilibrium constraint on k yields $k = 4.160$ (da^{-1}), which matches the shortest half-life in the literature. The data on the concentration of EPO from Maeda *et al.* [25] are shown with the solution $E(t)$ to (2.12) in Fig. 3.2.

The Figs. 3.1 and 3.2 show a fairly reasonable fit of the mathematical model to the experimental data. In Fig. 3.1, the data of Maeda *et al.* [25] tend to lie below the curve and show a slower recovery, while the data of Wadsworth [42] are significantly higher in the early part of the experiment (lacking data on the important first few days) and show a more rapid recovery to normal compared to the model. In Fig. 3.2, the EPO data of Maeda *et al.* [25] closely match the model for the first couple weeks, then again his subjects show a slower recovery. We note that these are two distinct experiments with small sample sizes, which complicate the comparisons of our model to the expected response of a normal human subject following a phlebotomy. The mathematical model shows that 90% of the erythrocytes lost from a blood donation are regenerated in slightly more than 30 days. This agrees with the statement in Wadsworth [42] (and often quoted by

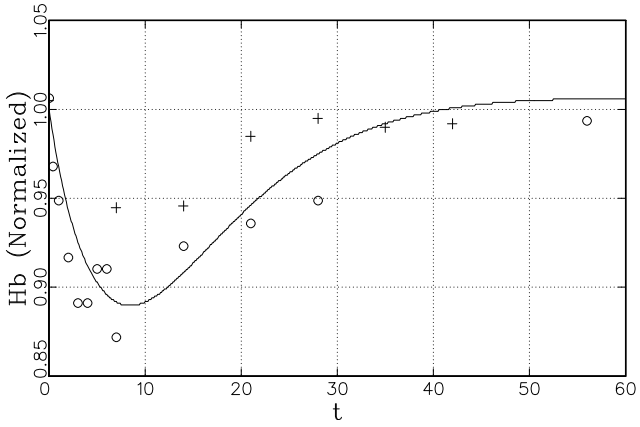

Figure 3.1: Simulation of Eqn. (2.12) with optimal parameters showing the concentration of hemoglobin following a blood donation with data of Maeda *et al.* (∘) and Wadsworth (+).

blood banks) "that recovery of haemoglobin concentration was completed within 3–4 weeks of the haemorrhage."

3.2 Simulation of the Age-Structured Model

With a set of parameters that match the data for the simplified model (2.12), we examined the effects of a variable velocity $V(E)$ on the system of partial differential equations, (2.1)–(2.9). Simulation of the complete age-structured model also allows a comparison of the model to the experimental measurements of blood reticulocytes. Our numerical technique parallels Sulsky [40], using the method of characteristics to follow the solution for fixed time steps. When the characteristic velocities $V(E)$ and W are one, then the aging of the structured populations move in step with time, which is why the age-structured model readily reduces to the system of delay differential equations. With $V(E)$ varying with E, the aging of the precursor population through its accumulation of hemoglobin and advancement to mature erythrocytes changes. Williams ([4], p. 436) claims that under extreme stress, the maturing stage of erythropoiesis is accelerated. Studies using radioiron [10, 16, 20, 32] show that anemic conditions can decrease transit time (time of maturation) in the bone marrow for precursor cells by over a day, and furthermore, the stress of blood loss results in early release

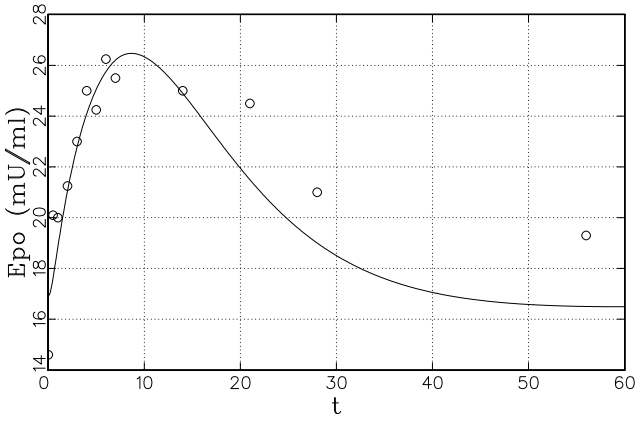

Figure 3.2: Simulation of Eqn. (3.12) showing EPO levels with data of Maeda *et al.* following a blood donation using the optimal parameters found by Eqn. (3.1).

of "shift reticulocytes." In the absence of EPO, the velocity of maturing, $V(E)$, should be zero, while at equilibrium it should be one. By assuming that at most maturation is accelerated by two days, we choose a velocity of maturation function of the form:

$$V(E) = \frac{\kappa_1 E}{\kappa_2 + E}, \tag{3.2}$$

where $\kappa_1 = 1.5$ and $\kappa_2 = 8.475$.

Below we outline the steps used for this numerical computation. The numerical simulation begins with a discretization of the density of precursor cells (number of cells/unit age, μ) and mature cells denoted

$$p(t_i, \mu_j) \equiv p_{i,j} \qquad \text{and} \qquad m(t_i, \nu_k) \equiv m_{i,k},$$

where $t_i = t_0 + ih$ for some step size in time h and $\mu_j(i)$ and ν_k for appropriate age-structure grids. With the variable velocity, the grid for precursor cells, $\mu_j(i)$, varies with time, t_i, which is also the reason that the density of the precursor cell population is studied. The values $p_{i,j}$ and $m_{i,k}$ are referred to as the age classes of cells at time t_i. In our simulation the normal human subject undergoes a phlebotomy at $t_0 = 0$. The initial age classes $\mu_j(0)$ and ν_k are separated by the stepsize h to give a uniform grid.

The age-structured model is easily solved to find its steady-state cell distribution. At equilibrium, $V(\overline{E}) = 1$ and with the assumption (2.11), then the precursor cell population has an exponential growth distribution until $\mu = \mu_R$, then the cell population remains constant until maturity. Divided into the discrete age classes, the initial density of precursor cells (number of cells/unit age, μ) is given by:

$$p_{0,j} = \begin{cases} P_0 e^{\beta \mu_j(0)}, & \mu_j(0) < \mu_R, \\ P_0 e^{\beta \mu_R}, & \mu_j(0) \geq \mu_R, \end{cases},$$

where $P_0 = S_0(\overline{E})$ is the initial density of new precursor cells, $\mu_R = 4$ (da), and $\mu_j(0) = jh$ for $0 \leq j \leq \mu_F/h = J_0$ and $\mu_F = 6$ for humans.

The steady-state distribution of mature cells is given by $\overline{m}(\nu) = P_0 e^{\beta \mu_R} e^{-\gamma \nu}$. At $t = 0$, the phlebotomy is assumed to reduce all age classes of mature erythrocytes by 8%. Thus, the initial distribution of mature erythrocytes:

$$m_{0,k} = 0.92 \overline{m}(\nu_k),$$

with $\nu_k = kh$ for $0 \leq k \leq \overline{\nu}_F/h$ and $\overline{\nu}_F = 120$ for humans. After the phlebotomy, the immediate effect on the hemoglobin concentration is no change, since the whole blood donation causes both plasma and erythrocytes to be lost. Hence, $Hb(0)$ is the same as the equilibrium value.

The method of characteristics is used for subsequent calculations of both the precursor and mature populations. The numerical routine begins by computing $V(E)$, using the value of E from the previous time step. This allows computation of the density of new precursor cells (number of cells/unit age, μ) by

$$p_{i,0} = S_0(E_{i-1})/V(E_{i-1}),$$

where i represents the index for time. The other precursor population densities are found by following the solutions along the characteristics. Thus, the new grid values, $\mu_j(i) = \mu_{j-1}(i-1) + hV(E_{i-1})$ for $1 \leq j \leq J_{i-1} + 1$ and precursor densities at the new grid points are

$$p_{i,j} = \begin{cases} p_{i-1,j-1} e^{\beta h V(E_{i-1})}, & \mu_j(i) < \mu_R, \\ p_{i-1,j-1}, & \mu_j(i) \geq \mu_R, \end{cases},$$

with special consideration for the case where $\mu_j(i)$ crosses μ_R having exponential growth up to μ_R and remaining constant afterwards.

The next step in the procedure is finding how many precursor cells enter the mature population. The precursor population densities are integrated

over this updated grid using the trapezoid rule to find how many cells are in this new population, including grid values with $\mu_j(i) > \mu_F$. The program finds the first $\mu_j(i) > \mu_F$. With this value of $j = J_i$, the final grid point is adjusted so $\mu_{J_i} = \mu_F$ and p_{i,J_i} is given by the weighted average between the values of p_{i,J_i-1} and p_{i,J_i} before the grid is adjusted. With this updated grid, the total new precursor population is computed using the trapezoid rule and is subtracted from the total computed before the grid was adjusted. The difference is the number of precursor cells entering the mature population, $m_{i,0}$, which satisfies the boundary condition (2.3).

The procedure for finding the populations in the mature age classes, $m_{i,k}$, is similar to that for the precursor age classes. However, since $W = 1$, the grid ν_k remains uniformly spaced with $\nu_k = hk$ for $0 \le k \le \nu_F(t_i)/h$, except for the final grid point, which depends on the boundary condition (2.4). The mature age classes at t_i satisfy

$$m_{i,k} = m_{i-1,k-1}e^{-\gamma h},$$

with each age class decaying exponentially at each time step.

The modeling assumption that a constant number of erythrocytes are destroyed for each time step affects the age of the oldest erythrocytes, $\nu_F(t)$, which determines the number of mature age classes. The numerical simulation takes the total number of mature erythrocytes from the previous time step and multiplies it by $e^{-\gamma h}$ to account for the general loss of erythrocytes from the destruction rate γ, then adds the new cells, $m_{i,0}$, entering from the precursor cell population. Next hQ of the oldest cells are removed with the program finding how many mature age classes remain, including any fractional remainder. Linear interpolation is used to find the new $\nu_F(t_i)$.

With the total mature population of erythrocytes, $M(t_i)$, known at t_i, Eqns. (2.6) and (2.8) are used to find the concentration of hemoglobin, $Hb(t_i)$. Then Eqn. (2.9) is integrated using an improved Euler's method to find the new concentration of EPO, $E(t_i)$. This completes a time step in the simulation and allows computation of all the key variables for any time by iterating the loop. Details on the accuracy and order of convergence of this algorithm and comparisons of integrating the partial differential equation to numerical integration of the equivalent delay differential equation when $V(E) = 1$ are provided at the end of this section.

Fig. 3.3 shows a simulation following a blood donation of the complete age-structured model with the variable velocity given in Eqn. (3.2), using a stepsize of $h = 0.02$, and compares it to the model given by Eqn. (2.12), where $V(E) = 1$. The figure shows that the concentrations of hemoglobin

and EPO vary only a few percent over the course of the simulation. If $Hb(t)$ and $E(t)$ are solutions with the variable velocity and $Hb_1(t)$ and $E_1(t)$ are solutions to (2.12), then the numerical data find that

$$\max_{0\le t\le 50} \frac{|Hb(t) - Hb_1(t)|}{Hb(t)} = 0.0057 \quad \text{and} \quad \max_{0\le t\le 50} \frac{|E(t) - E_1(t)|}{E(t)} = 0.018.$$

The velocity of aging reaches a maximum of $V(E) = 1.132$ at $t = 8.3$. Thus, a relatively large variation in the aging velocity produces relatively minor effects on the concentrations of hemoglobin and EPO. However, the changes do moderate the effect of the blood donation by increasing the minimum concentration of hemoglobin and having the recovery occur slightly earlier as seen by the left shift for the minimum of the graph in Fig. 3.3.

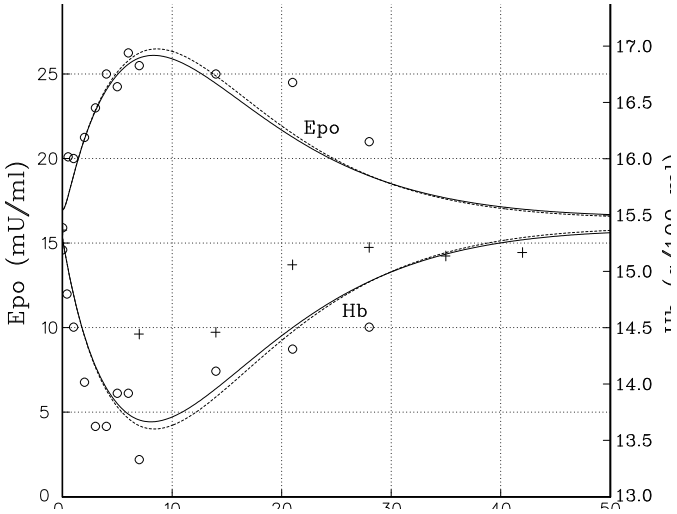

Figure 3.3: The solid curves show the age-structured model with variable velocity, while the dotted curves used $V(E) = 1$, which are equivalent to the graphs in Fig. 3.1 and 3.2. The data are shown for comparison.

3.3 Simulation and Bifurcation Analysis for a Rabbit with an Induced Hemolytic Anemia

Our next study examines the effects of including a variable velocity of aging to an age-structured model for an induced autoimmune hemolytic anemia in rabbits. Mahaffy *et al.* [26] fit their age-structured model to the experimental data of Orr *et al.* [31], where rabbits were given iso-antibodies

to their erythrocytes. In this paper we refine the values of the parameters to include more physiological data on rabbits and include the feedback control of EPO production (2.9) by the hematocrit given by Eqn. (2.6). Since the experimental data shows distinct oscillations, one might expect that the variable velocity of aging of the precursor cells would have a significant effect on the behavior of the model. Bélair and Mahaffy [3] showed that a variable velocity on a related model could have significant stabilizing effects. Thus, the experimental data of Orr *et al.* [31] for rabbits with an induced hemolytic anemia is fit using the algorithm for intgrating the partial differential equation with a variable velocity. The solution for the partial differential equation allows our model to be compared to data from Orr *et al.* [31] on the blood reticulocytes. With the same parameters, a numerical simulation of the age-structured model with $V = 1$ shows significantly higher amplitude oscillations, indicating a greater loss of stability as predicted. A linear analysis similar to Bélair and Mahaffy [3] of our model for rabbits with an induced autoimmune hemolytic anemia shows the stabilizing effect of the variable velocity of maturation.

A visual fit to the experimental data of Orr *et al.* [31] is performed using the numerical algorithm for the model that includes a variable velocity of maturation for the precursor cells. Many of the parameters in this model were set using physiological information from the literature before adjusting the few remaining parameters. A chapter by J. E. Smith [38] in *William's Hematology* provided useful information for determining the hematocrit function (2.6) for rabbits. The average hematocrit for rabbits is 41.2% with an erythrocyte count of $6.0 \times 10^6/\mu$l, so the normal $\overline{M}$ was taken to be 6.0. Thus, for rabbits the hematocrit function becomes

$$H(t) = \frac{M(t)}{M(t) + 8.56}.$$

J. Vacha [41] gave the formula $\overline{\nu} = 68.9m^{0.132}$, where m is the mass of the animal, for the lifespan of red blood cells for various animals, so assuming the experimental rabbits were between 0.5 and 1 kg, we use $\overline{\nu} = 65$ for the average lifespan of erythrocytes in rabbits. Orr *et al.* [31] stated that the mean red blood cell count for their anemic rabbits was about 75% of normal, which using human data would correspond to an equilibrium level of EPO of $\overline{E} = 70$ mU/ml. (We found no data on rabbit EPO concentration, and since this variable could readily be scaled, our choice of $\overline{E}$ was not important.) From the work of Bélair *et al.* [2] and Mahaffy *et al.* [26], we fixed the parameters $k = 6.65$, $K = 112,000$, and $r = 6.96$ in (2.9), where hematocrit, H, is used instead of hemoglobin.

In our simulation of the experimental data of Orr *et al.* [31], we adjusted the parameter γ, the equilibrium $\overline{H}$, and the time of maturation T, and had the computer program adjust the parameter a, the function $S_0(E)$, and the destruction rate Q to match the equilibrium values. The administering of antibodies to the erythrocytes in the experimental rabbits is assumed to effect primarily the random destruction rate γ in the model. Since the amount that this parameter increases was not measured directly, we used this as one of the parameters to be adjusted and found that $\gamma = 0.098$, about a 10-fold increase over normal, best fit the data. Since Orr *et al.* [31] claimed their experimental rabbits had about 75% of normal hematocrit, we varied $\overline{H}$ in a narrow range and found that $\overline{H} = 0.329$ (or $\overline{M} = 4.20$) best fit the experimental data. From an equilibrium analysis of (2.12), the $\dot{E}(t)$ equation gives $a = 23,281$. Under the assumption that $S_0(E)$ is linear with $S_0(E) = S_0'(\overline{E})E$, then simultaneously solving the steady-state equations for $\dot{M}(t)$ and $\dot{\nu}_F(t)$ give

$$e^{\beta\mu_R} S_0'(\overline{E}) = 0.00589 \qquad \text{and} \qquad Q = 0.000706.$$

We know that human erythrocytes take about 6 days to mature and that rat erythrocytes appear to mature more quickly, so we varied T, the time of maturation, in a narrow range to find the best fit to the data. We obtained $T = 4.33$ days from our simulations.

Fig. 3.4 shows simulations of (2.12) with $h = 0.05$ and the age-structured model with $h = 0.02$ and a varying velocity, $V(E)$, using (3.2) $\kappa_1 = 1.5$ and $\kappa_2 = 5$. This graph shows that a variable velocity of maturation has a significant stabilizing influence on the model. The bifurcation analysis below provides more details on why the variable velocity stabilizes the system. From a physiological perspective, our study suggests that by varying the rate of maturing for hematopoietic cell lines, an organism increases the stability of homeostasis for that type of cell. This added complexity in the feedback control is absent in the analysis of earlier models [2, 26].

xxx(Have Roland take a stab at this section.) The numerical simulation pointed to an error in the work of Mahaffy *et al.* [26] concerning the history used in the initial data for the delay differential equation, which is equivalent to the age-structured model with $V(E) \equiv 1$. The previous work used an initial history with $E(t) = 10$ for $-(T_1 + \overline{\nu}_F) \leq t \leq 0$. However, the history in the initial data for the delay differential equation must reflect the information contained in the age structure of the precursor and mature populations at $t = 0$. Since (2.12) only uses past information on $E(t)$, the initial data is found by choosing the appropriate levels of EPO needed to

generate the information stored in the age-structured populations. The age-structured populations at $t = 0$ are assumed to come from normal rabbits, which have a destruction rate $\gamma = 0.001$, thus their mature cells have a distribution $m(\nu) = m_0 e^{-0.001\nu}$ with $m_0 = 0.07176$ and $0 \le \nu \le \nu_F$. An appropriate equilibrium distribution can be made for the precursor cells. However, at $t = 0$, the experiment assumes that γ jumps to 0.065 and $\overline{M}$ shifts from 3.5 to 2.63. For $E(t)$ to reflect the distribution for $m(\nu)$ at $t = 0$ with $\gamma = 0.065$, we take $E(t) = 704e^{-0.064t}$, $-\overline{\nu}_F \le t \le 0$, which accounts for the difference in the values of γ before and after $t = 0$. A related extension accounts for the precursor population. Thus, the easier to simulate delay differential equation (2.12) may have a difficult history to analyze, while the computer simulation of the age-structured model has a more complicated algorithm with poorer convergence, but easier modeling interpretation.

Our numerical results suggest that a local analysis of mathematical model for a rabbit with an induced hemolytic anemia should yield a pair of eigenvalues with positive real part, which shift to all eigenvalues having negative real part when a variable velocity of aging is added. Bélair and Mahaffy [3] provide details for the stability analysis of the age-structured model for erythropoiesis presented in Section 2 (though not including the use of hematocrit for the negative feedback). The age-structured model is integrated along its characteristics, which are determined by the velocity of aging function, $V(E)$. With assumptions that $\kappa(\mu - \bar{\mu})$ is a δ-function with $\bar{\mu} = \mu_F$ and that $\beta(\mu, E)$ satisfies (2.11), the resulting system of integro-differential equations with a state-dependent delay has the form:

$$
\begin{aligned}
M(t) &= e^{\beta\mu_1} \int_0^{\nu_F(t)} V(E(t-\nu)) \frac{S_0(E(t-\nu-\tau))}{V(E(t-\nu-\tau))} e^{-\gamma\nu} d\nu, \\
\dot{E}(t) &= f(H(t)) - kE(t), \qquad (3.3) \\
\dot{\nu}_F(t) &= 1 - \frac{Q}{m(t, \nu_F(t))},
\end{aligned}
$$

where hematocrit is given by (2.6), τ satisfies the integral equation

$$\mu_F = \int_{t-\tau}^{t} V(E(r)) dr,$$

and

$$m(t, \nu_F(t)) = \frac{V(E(t-\nu_F(t)))S_0(E(t-\nu_F(t)-\mu_F))}{V(E(t-\nu_F(t)-\mu_F))} e^{\beta\mu_1} e^{-\gamma\nu_F(t)}.$$

This system is readily linearized about its unique equilibrium $(\overline{M}, \overline{E}, \overline{\nu}_F)$, and the resulting characteristic equation is given by

$$(\lambda+\gamma)(\lambda+k) - e^{\beta\mu_R} f'(\overline{M})(V_1 + V_2 e^{-\lambda T}) = 0, \tag{3.4}$$

where

$$V_1 \equiv \frac{V'(\overline{E})S_0(\overline{E})}{V(\overline{E})} \qquad \text{and} \qquad V_2 \equiv \frac{V(\overline{E})S_0'(\overline{E}) - V'(\overline{E})S_0(\overline{E})}{V(\overline{E})}.$$

A bifurcation diagram for the linearization of (3.3) is presented in Fig. 3.5. Let $A_1 = -e^{\beta\mu_R} f'(\overline{M})V_1$ and $A_2 = -e^{\beta\mu_R} f'(\overline{M})S_0'(\overline{E})$, then the characteristic equation (3.4) can be written

$$(\lambda+\gamma)(\lambda+k) + A_1 + (A_2 - A_1)e^{-\lambda T}) = 0, \tag{3.5}$$

where $A_1 \geq 0$ and $A_2 > 0$. A Hopf bifurcation occurs when (3.5) is solved for $\lambda = i\omega$, $\omega > 0$. Bélair and Mahaffy [3] show the existence of a Hopf bifurcation for $0 < \gamma < (A_2 - 2A_1)/k$, where

$$\omega = \sqrt{A_1 - \frac{k^2+\gamma^2}{2} + \frac{\sqrt{(k^2+\gamma^2-2A_1)^2 - 4((k\gamma+A_1)^2 - (A_2-A_1)^2)}}{2}}$$

and the critical delay or time of maturation is

$$T = \frac{1}{\omega}\arctan\left[\frac{\omega(k+\gamma)}{\omega^2 - (k\gamma + A_1)}\right] \quad . \tag{3.6}$$

where the appropriate branch of the inverse tangent is chosen.

3.4 Error Analysis of the Numerical Algorithms

The complicated nature of the algorithm for the partial differential equation model makes analytical studies of the error very difficult, so we performed two numerical studies to determine the accuracy and convergence of this algorithm. The first numerical study compares the algorithm for the partial differential equation model with $V(E) = 1$ to a Runge-Kutta method for the delay differential equation (2.12). Since these models are equivalent when $V(E) = 1$, then their numerical solutions should converge to the same unique solution. The second numerical study examines the global error of convergence of the algorithm for the partial diffferential equation model by varying the step size.

To numerically solve the delay differential equation model given by (2.12), a fourth order Runga Kutta method for ordinary differential equations is modified to include the delay history. For simplicity, a linear interpolation of the numerical data recorded from the simulation is used to approximate the discrete delay history for the model. The results of Rosen [34] show that the theoretical global order of convergence for delay differential equations is the sum of the order of convergence of the integration scheme and the order of convergence used to interpolate the history. Thus, our numerical scheme for solving (2.12) should be restricted by the linear interpolation of the history ($O(h)$). The numerical simulations of the model (2.12) show that the the maximum difference between subsequent solutions $Hb(t)$ and $E(t)$ found by halving the stepsize confirms the order of convergence of with global truncation error as $O(h)$. Furthermore, one finds that for step sizes $h \leq 0.02$ all solutions have less than 1% difference between the numerical simulations. Thus, sufficient accuracy of the numerical simulations is obtained with any step size below $h = 0.02$.

To verify the correctness of the algorithm described above for the partial differential equation model, the solutions from the algorithm with $V(E) = 1$ are compared to the solutions to the delay differential equation, which are of known accuracy. This comparison (using h = .01) we find that for $h \leq .01$, the results are within 0.00073 for $Hb(t)$ and .028 for $E(t)$. This indicates that the algorithm is consistent with the known results for $V(E) = 1$.

With $V(E)$ as defined in equation (3.2), we investigate the maximum difference for the solutions $Hb(t)$ and $E(t)$, $0 \leq t \leq 60$ while halving the stepsize. The results indicate Cauchy convergence corresponding to $O(h)$, which is to be expected since our code uses an Euler approach to integration. The data from this investigation is included in Table 2. When the stepsize is smaller than $h = .02$, all simulations agree to two significant digits for $Hb(t)$ and two significant digits for $E(t)$, indicating close proximity to the actual solution. For stepsizes below $h = .01$ computation time becomes significant. For this reason, $h = .02$ is used for all simulations.

i	h_i	Hb_d	E_d	$H_{d,i-1}/H_{d,i}$	$E_{d,1}/E_{d,2}$
1	0.2				
2	0.1	0.0285	0.1491		
3	0.05	0.0097	0.0538	2.938	2.771
4	0.025	0.0058	0.0338	1.672	1.592
5	0.0125	0.0026	0.0183	2.231	1.847
6	0.00625	0.0013	0.0094	2.000	1.947

We conclude that the algorithm is consistent with the simplified $V(E) = 1$ model and that it has global error of convergence $O(h)$. Furthermore, we find that for $h \leq .02$ the the solutions for different values of h have the required accuracy for our study.

Due to the complicated nature of this algorithm, traditional error analysis would be difficult. We investigated the maximum difference of $Hb(t)$ and $E(t)$, $0 \leq t \leq 60$, while halving the stepsize. The results indicate Cauchy convergence corresponding to $O(h)$, which is to be expected since our code uses an Euler approach to integration. When the stepsize is $h = 0.02$, all simulations agree to four significant digits for $Hb(t)$ and three significant digits for $E(t)$, indicating close proximity to the actual solution. The smaller number of significant figures for $E(t)$ appears to result from $E(t)$ being sensitive to small errors in Hb through the feedback function in (2.9) ($|df(\overline{H}b)/d(Hb)| \simeq 20$). For stepsizes below h = 0.01, computation time became significant, and the increases in roundoff error began to match the decreases in truncation error. For these reasons, h = 0.02 is used for all simulations.

4 Blood Donation Experiment and Discussion

The mathematical model for a phlebotomy seems to follow the data of Maeda *et al.* [25] and Wadsworth [42] fairly well. This suggests that the model could test different blood collection schemes or enhancements through EPO injections for obtaining more blood. However, the data that was used only provided a small sample with relatively large error bars, lowering the confidence in the mathematical model. This led the authors to wonder how well the model tracked an individual.

The authors were unable to obtain data on the individuals listed in the Maeda *et al.* [25] and Wadsworth [42] data, so with the help of the San Diego Blood Bank, two of the authors donated blood, then had their hemoglobin followed for eight weeks. The data in Fig. 4.1 show the results of this informal study, overlaying the simulation of our model. These data clearly do not show the general trend of the average data from the previous section, which was used to find the best parameters for our model. There remains the general trend at the beginning of the data for the hemoglobin to drop immediately following a blood donation, but this effect is very short lived. In fact, both authors saw a return to almost normal starting hemoglobin concentrations in 4 or 5 days. Soon the data follows an almost random

pattern with a mean of 14.66 and 15.10 (g/100 ml) for Mahaffy and Polk, respectively. (The standard deviation was 0.86 and 0.91 for Mahaffy and Polk, respectively.) The subjects of this study were not in a controlled experiment, so their diet and exercise regimes varied significantly (though measurements were taken at the same time each day).

The data in Fig. 4.1 show that our individual hemoglobin measurements are significantly more complicated than the data generated by the mathematical model (2.12). Since erythrocytes have the important role of carrying O_2 to all tissues in the body, one expects multiple controls with different time scales affecting the concentration of hemoglobin in the blood. While brain damage begins only minutes after the cessation of a blood supply, the process of erythropoiesis takes six days. Thus, other physiological controls on the blood supply are needed to adapt to sudden changes in demand for O_2 by the body tissues. As an example, one control discussed by Finch *et al.* [10] uses "shift reticulocytes" to rapidly introduce new erythrocytes to the body following a hemorrhage.

Environmental effects are clearly significant and dominate the process of erythropoiesis over shorter periods of time. For example, a phlebotomy often causes changes in the rate of hydration or urination in the subject, which directly effects blood plasma levels. In Fig. 4.1, the authors observed that the hemoglobin level dropped significantly for both participants following a day that included heavy exercise. Though initially this is counterintuitive, it becomes clear when thinking of blood as a viscous fluid. If the body needs more O_2 in the tissues, then it can accomplish this by decreasing the viscosity of the blood and having the blood flow more rapidly to the tissues, which it can do readily by shifting interstial fluid to the blood plasma. However, over a longer term the body would want to increase the concentration of erythrocytes, so that the heart would not have to pump as hard.

Several studies [30, 35, 44, 48] have been conducted comparing the blood of indigenous people living at high elevations. Amerindians (Quechua Indians) living in Peru and Himalayan natives (Sherpas) of Nepal both live at elevations exceeding 4000 m with the former being significantly more recent inhabitants to this elevation. Researchers have wondered how these people adapt to such extremes. Apparently, the Sherpas have similar hematocrit to average human populations by evolving an improved hemoglobin for carrying O_2. In contrast, the Quechua Indians have not adapted as well and have problems with polycythemia, which is a situation where the hematocrit is too high and patients have increased incidents of strokes, heart disease, and pulmonary edema. Both populations have more blood problems due to modest hypoxic hyperventilation and respiratory alkalosis. The studies of

these populations show additional complications in determining the controls of erythropoiesis.

The experiments tracked in Fig. 3.1 and 4.1 show the hemoglobin lower after 56 days, suggesting less than complete recovery after eight weeks, unlike the model. However, Mahaffy is a regular blood donor at the San Diego Blood Bank, and over a 40 month period (7/95–11/98) his hemoglobin averaged 15.2 (g/100 ml) with a standard deviation of 0.85, including a high of 17.6 (g/100 ml) and low of 13.7 (g/100 ml). (Note: The high of 17.6 (g/100 ml) followed six weeks of living at 2300m elevation.) Thus, there is tremendous variability of the hemoglobin levels even at "equilibrium."

The complicated mix of physiological controls, including external input of diet and exercise, makes a complete mathematical model very difficult at this time. For example, iron is a dietary element known to significantly effect the process of erythropoiesis (and is the primary reason Blood Banks require eight weeks between donations), yet iron's role is not included in the model. By including the effects of plasma volume and concentration dependent sensing of O_2, this study has improved the mathematical model of Mahaffy *al.* [26] for phlebotomized normal human subjects to better match data. The mathematical model works well describing the cummulative data of Maeda *et al.* [25] and Wadsworth [42] and agrees with an intuitive understanding for the control of erythropoiesis following a phlebotomy. Our numerical work demonstrates that the variable velocity of aging for the precursor cells has a minimal effect on the qualitative behavior of the model for normal human subjects, thus the simplified delay differential equation model is adequate for a basic understanding of erythropoietic controls following a phlebotomy. Still, the environmental factors dominate the changes in concentrations of hemoglobin and EPO, making our models inappropriate for determining better blood donation schemes.

Our comparative studies of the induced autoimmune hemolytic anemia for rabbits were particularly interesting. Mahaffy *al.* [26] simulated the experiments of Orr *et al.* [31] on rabbits with hemolytic anemia using a system of delay differential equations similar to (2.12). When we used the complete age-structured model and included the variable velocity of aging for the precursor cells, there was a significant increase in the stability of the mathematical model, as shown in Fig. 3.4. Further mathematical studies are needed to explain how this addition to the model effects stability. Biologically, this increased stability is clearly a favorable adaptation from an evolutionary point of view for maintaining homeostasis of erythrocytes.

Our numerical studies show that a simplified delay differential equation is much easier to examine, particularly when fitting parameters to the model.

However, the age-structured model is easier to interpret biologically. Both models for erythropoiesis provide clues for disease states centered around stem cells, and though they are inappropriate for improving blood donation schemes, they assist in the understanding of one major part of the regulatory process of carrying O_2 to the tissues.

Special thanks to the San Diego Blood Bank for their assistance with the hematocrit study of the authors. Their nursing staff was very cooperative, amiable, and informative for the duration of our experiment. Also, the authors recognize the assistance of Danielle Brown and Edward Trovato who were supported under the REU program of NSF by grant DMS-9208290.

References

[1] America's Blood Centers, 1998. Facts on Blood, www.americasblood.org/facts/frame.htm, Puget Sound Blood Center.

[2] J. Bélair, M. Mackey, and J. M. Mahaffy. Age-structured and two-delay models for erythropoiesis. *Math. Biosci.*, 128:317–346, 1995.

[3] J. Bélair and J. M. Mahaffy. Variable maturation velocity and parameter sensitivity in a model of haematopoiesis. *IMA Journal of Mathematics Applied in Medicine and Biology*, 18:193–211, 2001.

[4] E. Beutler, M. A. Lichtman, B. S. Coller, and T. J. Kipps. *William's Hematology.* McGraw-Hill, New York, 5$^{\text{th}}$ edition, 1995.

[5] S. Busenberg, K. Cooke, and M. Iannelli. Endemic thresholds and stability in a class of age-structured epidemics. *SIAM J. Appl. Math.*, 48:1379–1395, 1988.

[6] S. Busenberg and M. Iannelli. Separable models in age-dependent population dynamics. *J. Math. Biol.*, 22:145–173, 1985.

[7] O. Diekmann and J. A. J. Metz. On the reciprocal relationship between life histories and population dynamics. In S.A. Levin, editor, *Frontiers in Theoretical Biology. volume 100 Lecture Notes in Biomathematics*, pages 19–22. Springer-Verlag, Berlin and New York, 1994.

[8] C. D. R. Dunn. Cyclic hematopoiesis: The biomathematics. *Experimental Hematology*, 11:779–791, 1983.

[9] A. J. Erslev. Production of erythrocytes. In M.M. Williams, editor, *Hematalogy*, pages 389–397. McGraw-Hill, New York, 4$^{\text{th}}$ edition, 1990.

[10] C. A. Finch, L. A. Harker, and J. D. Cook. Kinetics of the formed elements of human blood. *Blood*, 50:699–707, 1977.

[11] J. A. Gatica and P. Waltman. A threshold model of antigen antibody dynamics with fading memory. In V. Lakshmikantham, editor, *Nonlinear Phenomena in Mathematical Sciences.* Academic Press, New York, 1982.

[12] J. A. Gatica and P. Waltman. A system of functional differential equations modeling threshold phenomena. *Appl. Anal.*, 28:39–50, 1988.

[13] R. R. Gordon and S. Varadi. Congenital hypoplastic anemia (pure red cell anemia) with periodic erythroblastopenia. *Lancet*, i:296–299, 1962.

[14] A. Grabosch and H. J. A. M. Heijmans. Cauchy problems with state-dependent time evolution. *Japan J. Appl. Math.*, 7:433–457, 1990.

[15] A. Grabosch and H. J. A. M. Heijmans. Production, development and maturation of red blood cells. A mathematical model. In D.E. Axelrod O. Arino and M. Kimmel, editors, *Mathematical Population Dynamics*, pages 189–210. Marcel Dekker, New York, 1991.

[16] R. S. Hill. Characteristics of marrow production and reticulocyte maturation in normal man in response to anemia. *J. Clin. Invest.*, 48:443–453, 1969.

[17] N. D. Kazarinoff and P. van den Driessche. Control of oscillations in hematopoiesis. *Science*, 203:1348–1350, 1979.

[18] E. A. King-Smith and A. Morley. Computer simulation of granulopoiesis. *Blood*, 36:254–262, 1970.

[19] J. Kirk, J. S. Orr, and C. S. Hope. A mathematical analysis of red blood cell and bone marrow stem cell control mechanisms. *British Journal of Haematology*, 15:35–46, 1968.

[20] S. Labardini, Th Papayannopoulou, J. D. Cook, J. W. Adamson, R. D. Woodson, J. W. Eschbach, and R. S. Hill. Marrow radioiron kinetics. *Haematologia*, 7:301–312, 1973.

[21] M. C. Mackey. A unified hypothesis for the origin of aplastic anemia and periodic haematopoiesis. *Blood*, 51:941–956, 1978.

[22] M. C. Mackey. Dynamic haematological disorders of stem cell origin. In J. G. Vassileva-Popova and E. V. Jensen, editors, *Biophysical and Biochemical Information Transfer in Recognition*, pages 373–409. Plenum Publishing Corp., New York, 1979.

[23] M. C. Mackey. Periodic auto-immune hemolytic anemia: An induced dynamical disease. *Bull. Math. Biol.*, 41:829–834, 1979.

[24] M. C. Mackey and J. G. Milton. Feedback, delays and the origin of blood cell dynamics. *Comments Theor. Biol.*, 1:299–327, 1990.

[25] H. Maeda, Y. Hitomi, R. Hirata, H. Tohyama, J. Suwata, S. Kamata, Y. Fujino, and N. Murata. The effect of phlebotomy on serum erythropoietin levels in normal healthy subjects. *Int. J. Hemat.*, 55:111–115, 1992.

[26] J. M. Mahaffy, J. Bélair, and M. Mackey. Hematopoietic model with moving boundary condition and state dependent delay: Applications in erythropoiesis. *J. theor. Biol.*, 190:135–146, 1998.

[27] J. A. J. Metz and O. Diekmann. *The Dynamics of Physiologically Structured Populations*, volume 68 Lecture Notes in Biomathematics. Springer-Verlag, Berlin, 1986.

[28] F. D. Moore. The effects of hemorrhage on body composition. *New Eng. J. Med.*, 273:567–577, 1965.

[29] A. Morley. Cyclic hemopoiesis and feedback control. *Blood Cells*, 5:283–296, 1979.

[30] G. Morpurgo, P. Arese, A. Bosia, G. P. Pescarmona, M. Luzzana, G. Modiano, and S. Krishnaranjit. Sherpas living permanently at high altitude: A new pattern of adaptation. *Proc. Natl. Acad. Sci. USA*, 73(3):747–751, 1976.

[31] J. S. Orr, J. Kirk, K. G. Gray, and J. R. Anderson. A study of the interdependence of red cell and bone marrow stem cell populations. *Brit. J. Haemat.*, 15:23–34, 1968.

[32] Th Papayannopoulou and C. A. Finch. Radio-iron measurements of red cell maturation. *Blood Cells*, 1:535–546, 1975.

[33] P. Ranlov and A. Videbaek. Cyclic haemolytic anaemia synchronous with pel-ebstein fever in a case of hodgkin's disease. *Acta Medica Scandinavica*, 174:583–588, 1963.

[34] I. G. Rosen. A discrete approximation framework for hereditary systems. *J. Diff. Eqn.*, 40:377–449, 1981.

[35] R. B. Santolaya, S. Lahiri, R. T. Alfaro, and R. B. Schoene. Respiratory adaptation in the highest inhabitants and highest sherpa mountaineers. *Respir. Physiol.*, 77:253–62, 1989.

[36] G. K. von Schulthess and N. A. Mazer. Cyclic neutropenia (CN): A clue to the control of granulopoiesis. *Blood*, 59:27–37, 1982.

[37] H. L. Smith. Reduction of structured population models to threshold-type delay equations and functional differential equations: A case study. *Math. Biosci.*, 113:1–23, 1993.

[38] J. E. Smith. Comparative Hematology. In E. Beutler, M. A. Lichtman, B. S. Coller, and T. J. Kipps, editors, *William's Hematalogy*, pages 77–88. McGraw-Hill, New York, 5^{th} edition, 1995.

[39] D. Sulsky. Numerical solution of structured population models: I Age structure. *J. Math. Biol.*, 31:817–839, 1993.

[40] D. Sulsky. Numerical solution of structured population models: II Mass structure. *J. Math. Biol.*, 32:491–514, 1994.

[41] J. Vacha. Red cell life span. In N. S. Agar and P. G. Board, editors, *Red Blood Cells of Domestic Animals*, pages 67–132. Elsevier, Amsterdam, 5^{th} edition, 1983.

[42] G. R. Wadsworth. Recovery from acute haemorrhage in normal men and women. *J. Physiol.*, 129:583–593, 1955.

[43] M. Wazewska-Czyzewska. *Erythrokinetics*. National Technical Information Service, Springfield VA, 1984.

[44] J. B. West. Respiratory and circulatory control at high altitudes. *J. Exp. Biol.*, 100:147–157, 1982.

[45] T. E. Wheldon. Mathematical models of oscillatory blood cell production. *Math. Biosci*, 24:289–305, 1975.

[46] T. E. Wheldon, J. Kirk, and H. M. Finlay. Cyclical granulopoiesis in chronic granulocytic leukemia: A simulation study. *Blood*, 43:379–387, 1974.

[47] H. E. Wichmann and M. Loeffler. *Mathematical Modeling of Cell Proliferation: Stem Cell Regulation in Hemopoiesis*. CRC Press, Boca Raton, 1988.

[48] R. M. Winslow, K. W. Chapman, C. C. Gibson, M. Samaja, C. C. Monge, E. Goldwasser, M. Sherpa, F. D. Blume, and R. Santolaya. Different hematologic responses to hypoxia in sherpas and quechua indians. *J. Appl. Physiol.*, 66:1561–1569, 1989.

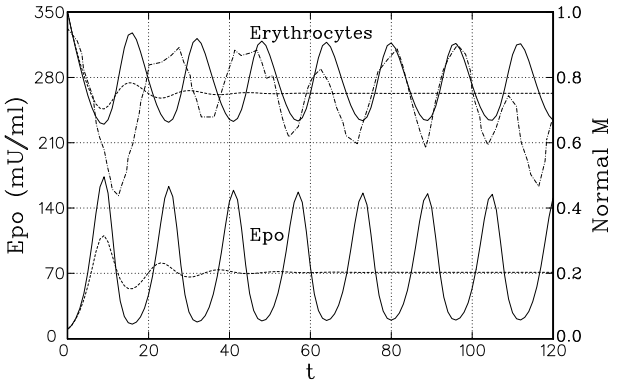

Figure 3.4: The dashed curve shows the age-structured model with variable velocity, while the solid curve used $V(E) = 1$. The data from Orr *et al.* is shown (dot and dash curve) and has similar oscillatory behavior to the $V(E) = 1$ curve.

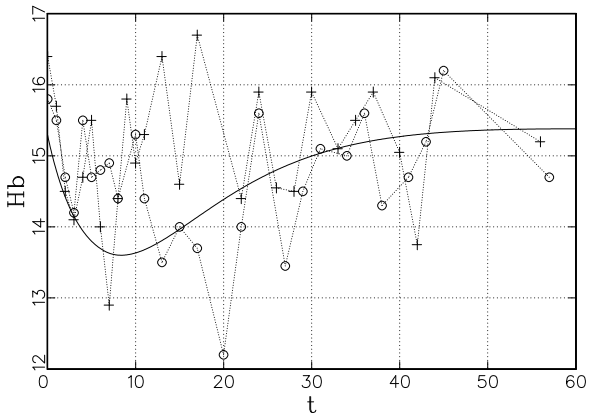

Figure 4.1: The solid curve shows the level of hemoglobin following a blood donation predicted by the model in Section 3. The data with $\circ$ are from the author Mahaffy, while the data with $+$ are from the author Polk after a blood donation at $t = 0$.